Sol-gel synthesis and *in vitro* characterization of bioactive glass ceramics using rice husk ash waste material

A Thesis Submitted in Partial Fulfillment of the

Requirements for the Degree of

Bachelor of Technology

by

Sanjeet Kumar

(Roll No: 10508028)

Supervisor:

Dr. JAPES BERA

DEPARTMENT OF CERAMIC ENGINEERING

NATIONAL INSTITUTE OF TECHNOLOGY, ROURKELA, ORISSA

JANUARY, 2009

ACKNOWLEDGEMENTS

With deep regards and profound respect, I avail this opportunity to express my deep sense of gratitude and indebtedness to Prof. Japes Bera, Department of Ceramic Engineering, N. I. T. Rourkela, for introducing the present research topic and for inspiring guidance, constructive criticism and valuable suggestion throughout this research work. It would have not been possible for me to bring out this project report without his help and constant encouragement. I wish that he will keep in touch with me in future and will continue to give his valuable advice.

I would like to express my gratitude to Prof. Santanu Bhattacharyya, Head of Ceramic Engineering Department, for his cooperation in one way or the other. I wish to record my thanks and gratitude to him for his valuable suggestions and encouragements at various stages of the work.

I am also grateful to Prof. S. K. Pratihar, Department of Ceramic Engineering, whose vast knowledge in the field of science and technology has enlightened me in different areas of this experimental research work. His deep sense of appreciation and dedication to research has been a constant source of inspiration to me.

It was a nice and memorable association with all the stuff of my department. I wish to give them my heartfelt thanks for their constant help.

Above all, I thank our saving Bajarang bali for giving me all these people to help and encourage me, and for the skills and opportunity to complete this report.

Date: 07.05.2009 (Sanjeet Kumar)

INTRODUCTION

Glass-ceramic s materials share many properties with both glass and more traditional crystalline ceramics. It is formed as a glass, and then made to crystallize partly by heat treatment. . Bioactive glass-ceramics describes the beneficial or adverse effects of glass-ceramic with living tissue , when placed in body.

Bioactive glasses and glass-ceramics are more and more studied because of their surface chemical reactivity when in contact with body fluids [1–3]; by a complex mechanism of ions leaching and partial dissolution of the glass surface, the precipitation of bone-like apatite from the solution provides a strong chemical bonding with tissues. Since bioactive glasses and glass-ceramic are brittle materials, they are especially used in the field of small bone defects reconstruction, or as coatings on inert substrates for load-bearing prostheses.

Since the discovery of bioglass by Hench et al. [4] in the early 1970s, various types of ceramic, glass and glass–ceramic have been proposed and used as bone replacement biomaterials [5-7]. Specifically, these biomaterials have found clinical applications as coating for prostheses, bone filler, vertebral substitution and, in a porous form, as bone substitutes [8-15]. Most of them are based on the SiO2–P2O5–CaO–Na2O system. Bonding between bioactive glass or glass–ceramic and the surrounding tissues takes place through the formation of a hydroxyapatite layer, which is very similar to the mineral phase of bone. When the bioactive glass is placed in contact with physiological fluids, this layer is formed through a complex ion-exchange mechanism with the surrounding fluids, known as bioactivity.

This biologically-active layer of hydroxyapatite can form on the surface of glasses having a wide compositional range, and is considered as self by the surrounding living tissue; its presence is widely recognized to be a sufficient requirement for the implant to chemically bond with the living bone. Kokubo et al. [16] proposed the Tris-buffered simulated body fluid (SBF) for the in vitro study of bioactive glass and glass–ceramic, since its ion concentration is almost equal to that of human blood plasma. Since then, in vitro tests in SBF have been widely used as preliminary tests on new candidate materials showing bioactive properties. The ion leaching phenomenon involves the exchange of monovalent cations from the glass, such as Na+ or K+, with H3O+ from the solution, and thus causes an increase in the pH of the solution. It is known that osteoblasts prefer a slightly alkaline medium [17, 18], but it is also known that severe changes in pH can inhibit osteoblast activity and cause cell necrosis or apoptosis [19-21].

Different bioactive glass and glass ceramics have been synthesized in order to get desired mechanical, chemical properties by obtaining required microstructure. Some of common components used are Na_2O, CaO, P_2O_5, SiO_2 for synthesis of 45S5 and S53P4. In addition to these above components, varying composition of K_2O, MgO , B_2O_3 are used to get 13-93, 3-04, 18-04, 23-04. There are some other glass and glass ceramics which also include ZnO, Ag and Al_2O_3.

In current study of bioactive glass ceramic we are using rice husk ash as raw material for synthesis of silica, which is amorphous in nature. It is cheap, easily available source with high content of silica.

Literature Review

Thousands of years ago human discovered that clay could be irreversibly transformed by fire into ceramic pottery which stored grains for long time with minimal deterioration. During last 100 years another revolution has occurred in the use of ceramic to improve the quality of human. The revolution is the development of specially designed and fabricated ceramics for repair and construction of diseased, damaged or worn out parts of body. Ceramics used for this purpose is called BIOCERAMICS.

Types of bioceramics-Tissue interface

All implanted material elicit a response from host tissue. The response occurs at tissue–implant interface. There are four general type of tissue–implant response. When the implant is toxic, host tissue dies. Whereas, biologically inert implant are encapsulated by fibrous capsule by tissue. This prevents the interaction of implant with host. Another type of interface is bioactive in which tissue forms bonding with implant. There are some implant which are replaced by tissue in due course of time. The implant get dissolved into physiological fluid. The restriction with this implant is that its composition should be very close to body fluid.

Types of bioceramics-Tissue attachments

The mechanism of attachment of tissue to an implant is directly related to the tissue response at tissue–implant interface. There are four types of bioceramics each with a different type of tissue attachment.

The related chemical activity of different types of bioceramics depends on rate of bonding with bone. The relative level of reactivity of an implant also influences the thickness of the

interfacial layer between material and tissue. Type 1, nearly inert, implant form a non adherent fibrous layer at the interface. However if these implant are loaded such that interfacial movement occurs, the fibrous capsule can become several micrometer thick and the implant loosens very quickly leading clinical failure.

Porous ceramic and HA coating, a type 2 bioceramics, on porous metal are developed to prevent loosening of implants. The growth of bone into surface porosity provides a large interfacial area between the implant and its host. This method of attachment is often called BIOLOGICAL FIXATION. It is capable of withstanding of more stress than type 1 implant which achieve only morphological fixation. A limitation of type 2 porous implant is the necessary for the pores to be at least 100 micrometer in diameter. Large pore size is required so that capillaries can provide a blood supply to the ingrown connective tissue. If pores < 100 micrometer then even if the micro movements occur, Capillary can be cut off leading to tissue death. When the porous implant is metal, interfacial area can provide a focus for corrosion of implant and loss of metal ion into the tissue, which may cause a variety of medical problem. Coating of these porous metals with HA, diminishes some of these limitations. The Ha coating also improve the rate of bone growth into pores. But coating dissolves with time which limits its effectiveness.

Bioactive implant (type 3) is another approach to achieve interfacial attachments. This is intermediate concept between resorbable (type 4) and bioinert behavior. A bioactive material undergoes chemical reaction in the body, but only at surface leading to bonding of tissue at the interface. Thus a bioactive material is defined as “a material that elicits a specific biological response at the interface of material which results in the formation of a bond between the tissue and the material. The bioactive concept has been expanded to include many bioactive materials with a wide range of bonding rate and thickness of interfacial bonding layer. These include bioactive glass, bioactive glass-ceramics, dense synthetic hydroxyapatite, bioactive composites, bioactive coating. The time dependence of the bonding, strength of bond, the mechanism of bonding, the thickness of bonding zone, and the mechanical strength differ for various materials.

Type 4 is resorbable implants which are designed to degrade gradually with time and be replaced with natural tissue. A very thin or non existent interfacial thickness is the final result. This is the optimal solution to problem of interfacial stability. It leads to the generation of tissue instead of their replacement. The difficulty is meeting requirement of strength and short

term mechanical performance of implant while regeneration of tissue is occurring. The resorption rate is must be matched to repair rate of body tissue but some material dissolve too slowly and others too fast. Since large quantities of materials being handled by cells so the constituents of resorbable implants should be metabolically acceptable.

Tissue response to implants

To understand the way in which tissue respond to an implant it is necessary to understand the nature of tissue at the interface and the significance of any alterations seen there. The significance of such changes will vary with the material and will vary with the material and will be governed both by their severity and by their persistence, a transient change or a continuing one may both appear to be identical shortly after implantation.

Every organ in body is made up from a combination, in varying proportion of four tissue types: Epithelium, Muscle, nervous and connective tissue. Epithelial tissue secretes a wide variety of substance either through ducts or into blood stream. Glands are made of this tissue. Muscle tissue is found wherever movement is required. Nervous tissue is responsible to transmit signal between outside world, the brain and other parts of body. Fourth, connective tissue is named as such because it connects all other. It includes blood supply to and from organs. No organ in body is without connective tissue and it is with connective tissue that ceramic biomaterials interact.An inflammatory response will always be there immediately after surgery while the damaged tissue, blood clot, and the bacteria introduced at the time are removed. The reddening and swelling occurs increasing the blood supply produced by the chemical released by damaged tissue. With the blood reaches cell involved in repair process. These include many cell known as phagocytes, for their ability to digest and remove foreign material. It is the presence of these phagocytes at any time other than immediately post-implantation, which can indicate problems with a material or an implant.

COMPOSITION

Composition of various glass and glass-ceramic were studied in order to choose appropriate composition for our purpose. While going through different journals, following observations were made which reflects the effects of various chemicals on bioactivity of glass and glass-ceramics.

Some of standard composition of bioactive glass and glass-ceramics are in Table1.

NAME	Na_2O	K_2O	MgO	CaO	B_2O_3	P_2O_5	Al_2O_3	SiO_2	ZnO
45S5	24.5	0	0	24.5	0	6	0	45	-
S53P4	23	0	0	20	0	4	0	53	-
13-93	6	12	5	20	0	4	0	53	-
4-Mar	5	15	6	22.5	0	1	0	50.5	-
18-04	15	0	4.5	20	2	4	0	54.5	-
23-04	5	11.25	4.5	20	2	1	0	56.25	-
H2-02	6	11	7	22	1	2	0.5	53	-

All the above compositions are in wt%

CEL-2	15	4	7	26	_	3	-	45	-
55S	-	-	-	41	-	4	-	55	-
H	24.3	-	-	26.9	-	2.6	-	46.2	0
HZ5	23.4	-	-	25.9	-	2.5	-	44.4	3.8
HZ10	22.5	-	-	4.8	-	2.4	-	42.5	7.8
HZ20	20.5	-	-	22.6	-	2.2	-	38.8	15.9

There are in mole%

Effect of Ag_2O and use of sol-gel method: In recent studies [22, 23] ntroduction of Ag_2O into bioactive glass compositions aimed at minimizing the risk of microbial contamination through the potential antimicrobial activity of the leaching Ag+ ions has been reported. It has been shown that a bioactive glass composition doped with Ag2O elicits rapid bactericidal reaction. The production of materials via the sol–gel process allows for tailoring of the textural characteristics of the matrix in order to obtain a controlled Ag+ delivery system.

Effect of B_2O_3: The introduction of B_2O_3 into the $CaO–SiO_2$ system is expected to enhance the bioactivity, for more soluble boric compounds increase the supersaturating of Ca ions in the SBF solution and water-corrosive borosilicate glass forms Si–OH groups that act as nucleation sites for the apatite layer [24].

Effect of ZnO: Zn-substituted bio-glasses create a template for osteoblast proliferation and differentiation that could be encouraged by the interaction between the Zn and inorganic phosphate at the surface of the bioactive glass. Addition of Zn is beneficial for cell attachment and for maintaining the pH of SBF within the physiological limit by forming zinc hydroxide in the SBF solution. In vitro biocompatibility assessments indicate that substitution of limited amounts of Zn in the bioglass system stimulates early cell proliferation and promotes differentiation.

Textural properties influencing bioactive behavior: It was reported that textural properties (pore size, pore volume, pore structure) of biomaterials may have complex influences on the development of the apatite layer. Increasing the specific surface area and pore volume of bioactive glasses may greatly accelerate the apatite formation and therefore enhance the bioactive behavior [25].

Synthesis:

In general, bioglasses can be formed by the additional method, which is regarded as simple and suitable for mass production [26, 28]. However, this method is limited by the evaporation of the volatile component P2O5 during high-temperature processing. The sol–gel technique is an alternative approach to fabricating bioglasses that has been widely studied in recent years [29,30]. The advantages of the sol–gel process are well known: the process takes place at low temperatures, and gives homogeneous mixtures in the final glass composition. It has been proven that commercially available glass compositions, e.g. 45S5, 58 S and 64 S, can be synthesized by the sol–gel method [31–34].

EXPERIMENTAL

1. Synthesis of Silica from Rice husk

Fig.1 shows the schematic process for extraction of silica from rice husk. Rice husk (RH) was collected from a rice mill in Rourkela, India. The RH was separated from rice grain by air blowing and washed with tap water for several times till all the blackish impurity floating on water was completely removed. The rice husk was then dried at 110^{O}C for 8 h. The dried husk was burning at 700°C for 6 h for complete combustion by which all volatile material is removed and ash was obtained. This ash contained more than 96% silica.

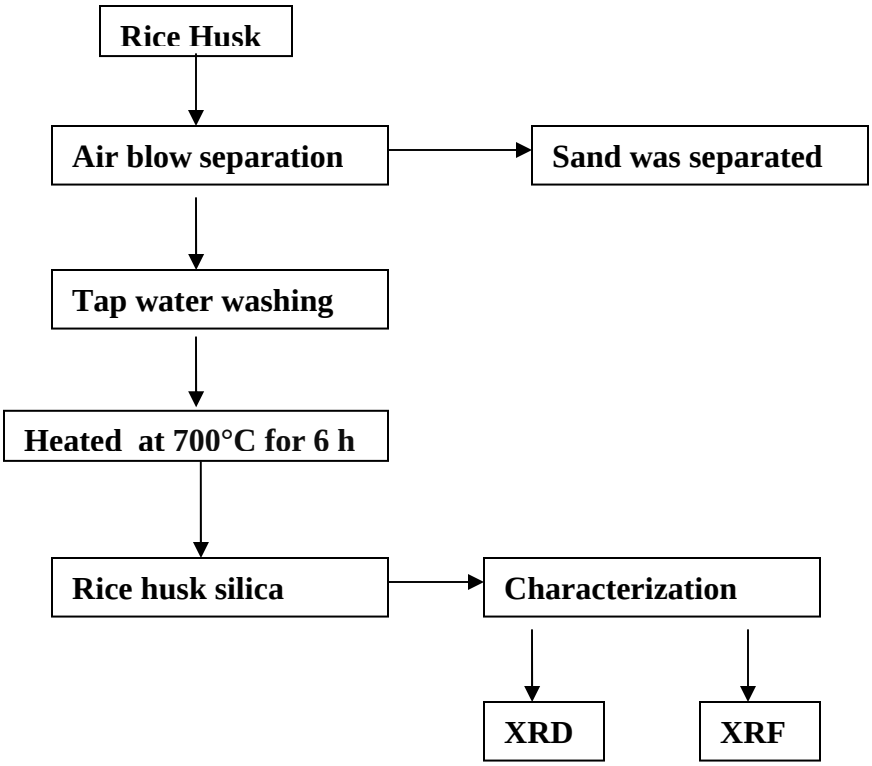

Fig.1 Flowchart for synthesis of silica from rice husk

2. Synthesis of glass-ceramic gel powder

2.1 Synthesis of glass-ceramic gel powder from rice husk silica (RHS)

The composition of gel powder to be synthesized was taken as SiO_2- 50mol%, Na_2O-25mol%, CaO-25mol%. RHS was taken as source of silica whereas NaOH and $Ca(NO_3)_2.4H_2O$ were the sources of Na_2O and CaO respectively.

RHS – 2.5 gm

NaOH—1.6634 gm

$Ca(NO_3)_2.4H_2O$ – 4.9198 gm

HNO3 (conc)—95 ml

First of all, 2.5 gm of RHS was taken and corresponding amount of NaOH and $Ca(NO_3)_2.4H_2O$ were obtained. Estimated NaOH and $Ca(NO_3)_2.4H_2O$ were dissolved in 20 ml and 30 ml of deionized water in beaker which gave clear solutions. NaOH solution was warmed RHS was added into it in warm condition only and volume was made 60 ml by adding water. The boiling was continued for 1 hr while volume was maintained upto 60 ml mark of beaker regularly at around time interval of 15 min. After 1 hr of boiling, RHS dissolved completely. Then this solution was filtered and we obtained 50 ml of Sodium silicate solution.

Estimated amount of $Ca(NO_3)_2.4H_2O$ solution was prepared by dissolving it in 30 ml of deionized water. Then 15 ml of HNO3(conc) was added in $Ca(NO_3)_2.4H_2O$ solution, which was kept in stirring condition, followed by addition of Sodium silicate solution drop wise very slowly. At intervals, HNO_3(conc) was added for neutralization and to avoid precipitation. When concentration of HNO3was high in solution, its fume were rising up and some reaction occurred with Sodium silicate solution drop falling from burette. From earlier trial it was observed that just before precipitation, the stirring sound changed suddenly. So, in final gel powder preparation it was completely avoided by adding HNO3 at proper interval. Initially, addition rate of Sodium silicate solution was 5 ml per min. At the end when 7-8 ml of Sodium silicate solution was left in beaker, rapid addition was made. By the time gelation started and took 45 min for completion after complete addition of Sodium silicate solution. Then it was left for 3 days at 70^oC for ageing so that glass network formation is optimized. Then it was dried at 150^oC for 2 days.

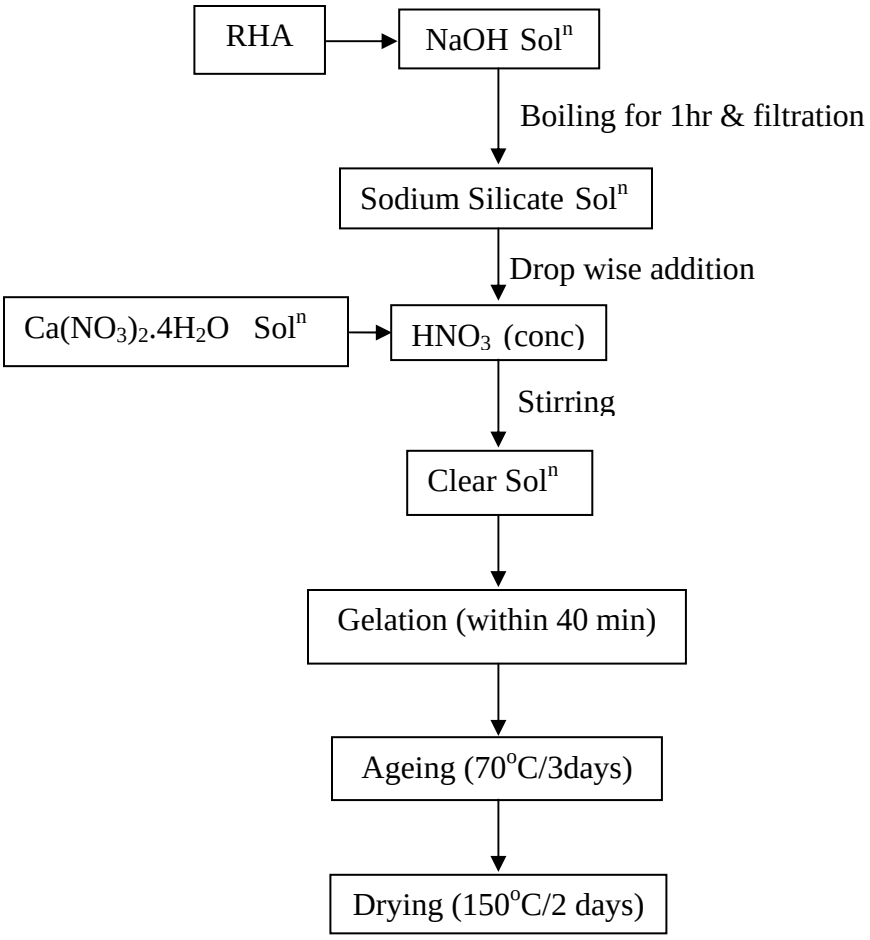

Fig.2 Flow chart of glass-ceramic gel powder from RHS

2.2 Synthesis of gel powder from TEOS

For 20 gm of sample

TEOS solution --- 38cc

NaNO3 --- 14.1376 gm

Ca(NO3)2.4H2O --- 19.6792 gm

0.1 M HNO3 --- 78.2 ml

Required amount of TEOS was taken and poured into 78.2 ml of 0.1 M HNO3 and kept for 40 min in stirring condition to get clear solution. Then $Ca(NO_3)_2.4H_2O$ was added and stirred for 45 min till it dissolved. Finally, NaNO3 was added in stirring condition and took 45 to dissolve completely. Then solution was left in stirring for 4 hrs after which turbidity started appearing indicating network formation. Then stirring was stopped and gelation was complete in 1 hr.

The gel was kept at 70^{o}C for 3 days followed by 150^{o}C for 2 days for edging and drying respectively.

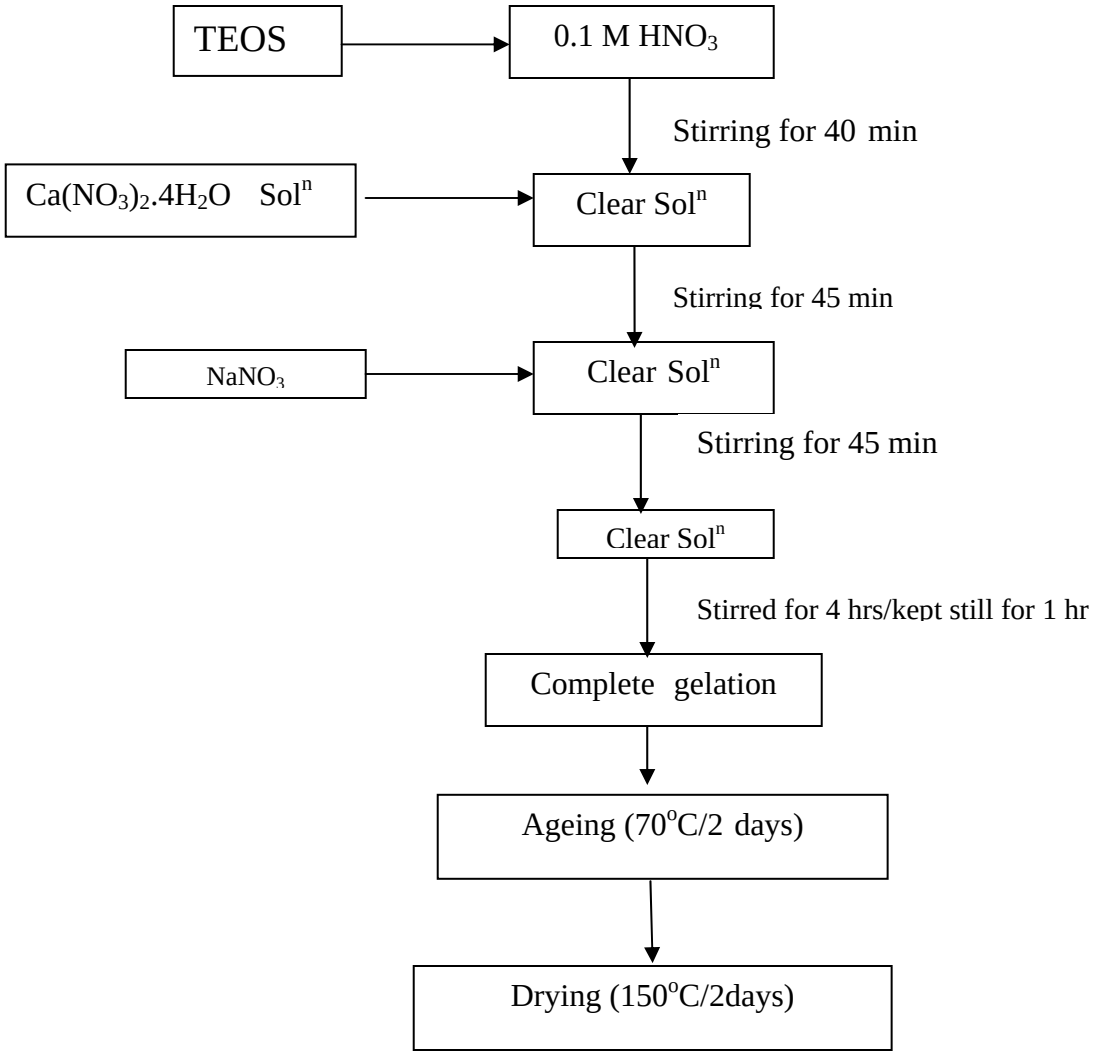

Fig.3. Flowchart of synthesis of gel Powder using TEOS silica

Preparation of glass-ceramics body

Fig. 4 is schematic flowchart for the preparation of glass-ceramics body. After the preparation of gel powder, it was well ground and DSC-TG analysis of both sample were done upto 1000^{o}C. The information of DSC-TG directed for calcinations of samples at 700^{o}C for 2 hrs. Then XRD analysis of calcined material was done which evidenced the presence of crystalline phase and its conversion to glass-ceramics from glass. This calcined powder sample was then pelletized.1 gm of each calcined powder was taken and pressure of 2.5 ton was applied with soaking time of 2min. Average diameter was about 15 mm. Then these pellets were sintered at

800^{o}C for 2hrs. The average BD and AP of RHS based sintered pellets was 1.5147gm/cc and 20.2 %, the respective value for TEOS based sintered sample was 1.7823gm/cc and 12.9%.

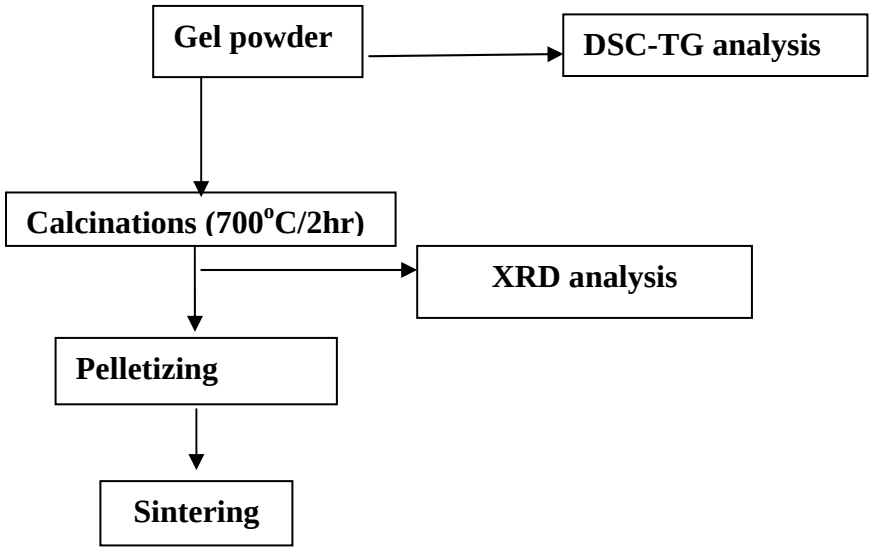

Fig.4. Flowchart for the preparation of glass-ceramics body

In vitro Bioactivity test:

SBF is known to be a meta stable buffer solution and even a small, undesired variation in preparation step and storage temperature may drastically affect the phase purity and high temperature stability of produced HA powder as well as kinetics and precipitation process.

Merc-grade NaCl (99.5%), $NaHCO_3$(), KCl (99.0%), $MgCl_2.6H_2O$ (99%), $Na_2HPO_4.2H_2O$ (99.5%), $CaCl_2.2H_2O$ (99%),Na_2SO_4 (99.5%), Tris buffer (99.5%) and HCl were used in the preparation of SBF in this study. Table 1 shows the reagents required and order of addition. SBF solution was prepared by adding appropriate amount of above chemical in deionized water. Reagents were added one by one after each reagent was completely dissolved in 700ml of water in the order given in table. A total of 62 ml of 1M HCl was consumed for the preparation of 1L of SBF solution. About 3 ml of 1MHCl was added after dissolving each reagent to adjust pH. The remaining part of acid was used in titration following the addition of tris [(hydroxymethyl)aminomethane] while temperature was maintained at 37^{o}C and pH was brought to 7.4. During the titration process deionized water was also added to make the volume 1 liter.

Table 1 Chemical composition of SBF solution

Order	Reagent	Amount (gpl)
1	NaCl	6.547
2	NaHCO3	2.268
3	KCl	0.373
4	Na2HPO4.2H2O	0.178
5	MgCl2.6H2O	0.305
6	CaCl2.2H2O	0.368
7	Na2SO4	0.071
8	(CH2OH)3CNH2	6.057

Samples, TEOS and RHA synthesized, were placed in SBF with its surface vertical. This position allowed both surfaces to interact with SBF and avoided settling of ions on its surface which could be possible in horizontal position. The container was closed and kept in incubator at 37^{o}C. After 3days, 7days, 14days and 21 days samples were taken out and soaked in water for 5 hrs and cleaned with caution so that surface is not damaged. Then it was kept in air tight dessicator. Further, XRD and SEM and FTIR analysis was done.

In vitro degradation test:

In order to study the dissolution/reprecipitation features of glass-ceramics, Tris buffer solutions was chosen because: Tris is the plain buffering agent used in most SBF preparations [35]; Tris solutions, whose use has been suggested also by Hench [36], do not contain ions and thus represent, for a bioactive material, maximum solubility and minimum reprecipitation activity.

Tris solution:

Merck made Tris was dissolved in distilled water to obtain a concentration of 6.1 g L^{-1}. The solution pH was lowered to 8 by acidifying with a solution of 1 M HCl.

Result and Discussion:

Characterization of rice husk silica

After cleaning of rice husk by air blowing and tap water washing, rice husk was dried. A sample of this was taken for XRD. After calcination of this sample at 700^{o}C for 6h, XRD (fig.5) and XRF (Table2) was done. Crystallite size of ash was found to be smaller than that in case of rice husk as peak in XRD pattern of ash is broader than rice husk. The temperature so chosen is as because calcining at temperature below it, volatile materials don't go off completely. Calcination at temperature above it causes silica to react with other constituent decreasing percentage amount of silica. Since percentage of silica, which is amorphous in nature, is increased, this caused the broadening of peak in rice husk ash.

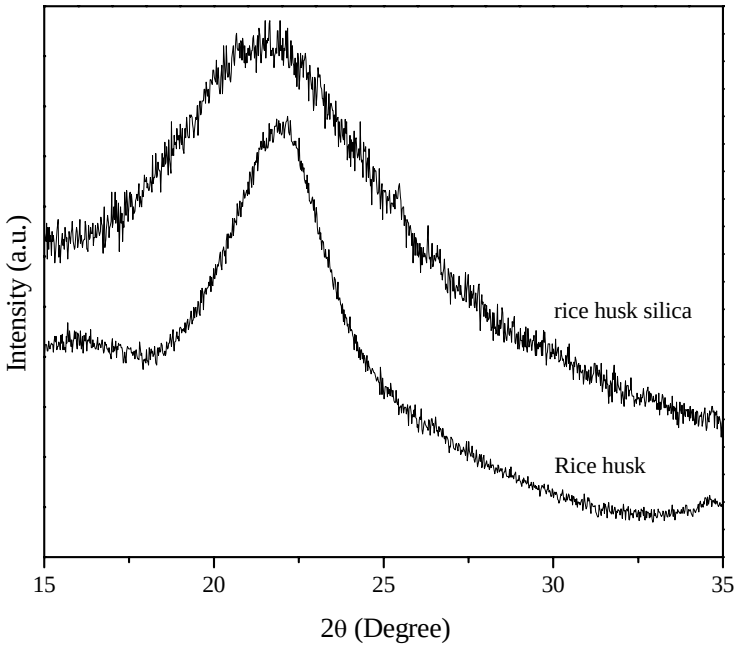

Fig.5. XRD pattern of RHS and rice husk

Table 2 XRF analysis of rice husk and rice husk silica

Oxides	Raw rice husk	Rice husk silica
SiO2	93.140	96.009
SO3	0.397	-
K2O	0.433	0.856
CaO	3.805	2.221
Fe2O3	1.540	0.571
ZnO	0.154	0.066
Mn2O3	0.53	0.278

Thermal decomposition behavior

Fig.6 shows simultaneous TG-DSC curves for RHS based (NS-BGC), Soda-lime- silicate gel powder. There are three major weight loss in the temperature range, up to 200^{o}C then 200^{o}C-500^{o}C then 500^{o}C-800^{o}C. These weight losses correspond to mainly different endothermic reactions as shown by DSC curve. First weight loss of about 12% is due to loss of gel water which corresponds to huge endothermic peak in DSC at 120^{o}C. There is such endothermic peak about 227^{o}C which accompanied with no weight loss behavior that may be due to structural change occurring in gel. Gel is amorphous, if some crystallization of phases occur then that will be accompanied with endothermic peak. This phenomenon can be confirmed after explaining XRD analysis. The weight loss in the range 200^{o}C to 500^{o}C range, seems accompany with some exothermic behavior. Weight loss (about 6.2%) is due to decomposition of nitrate compound and residual water of gel. The weight loss in the range 500^{o}C to 800^{o}C corresponds to 35.8%. This is only due to decomposition of sodium nitrate and calcium nitrate. The weight loss was completed at 800^{o}C.

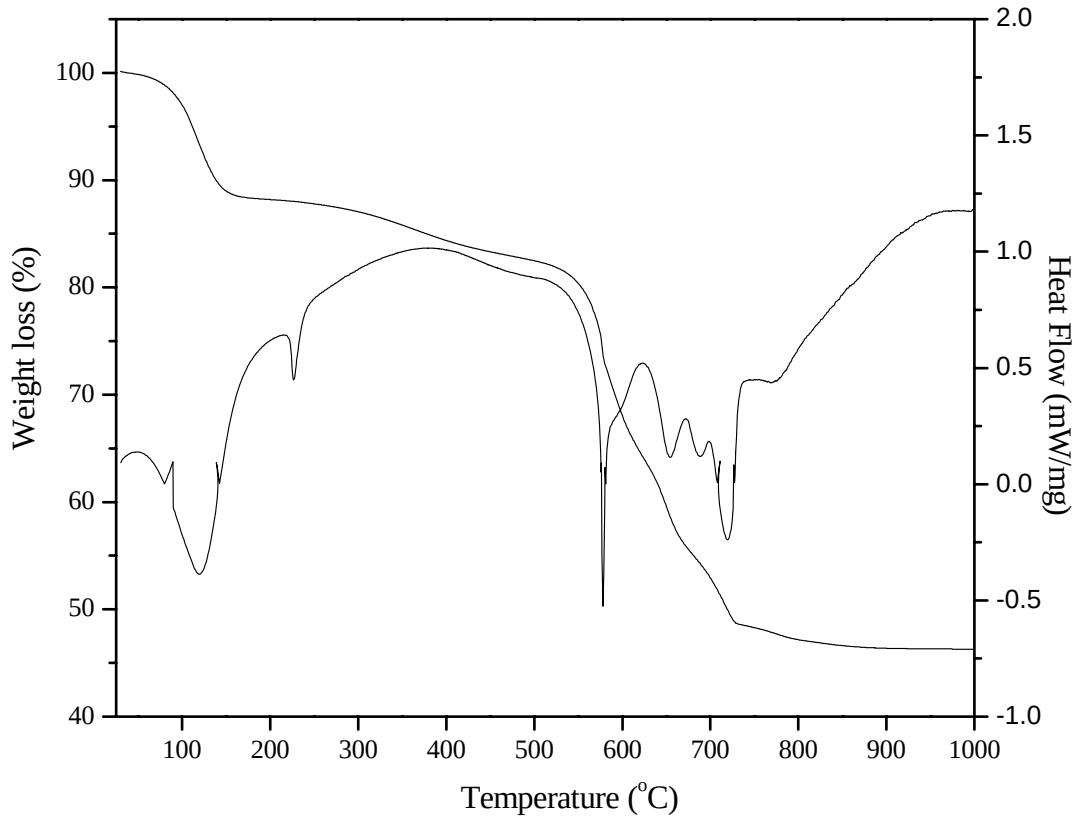

Fig.6. DSC-TG plot of NS-BGC gel powder

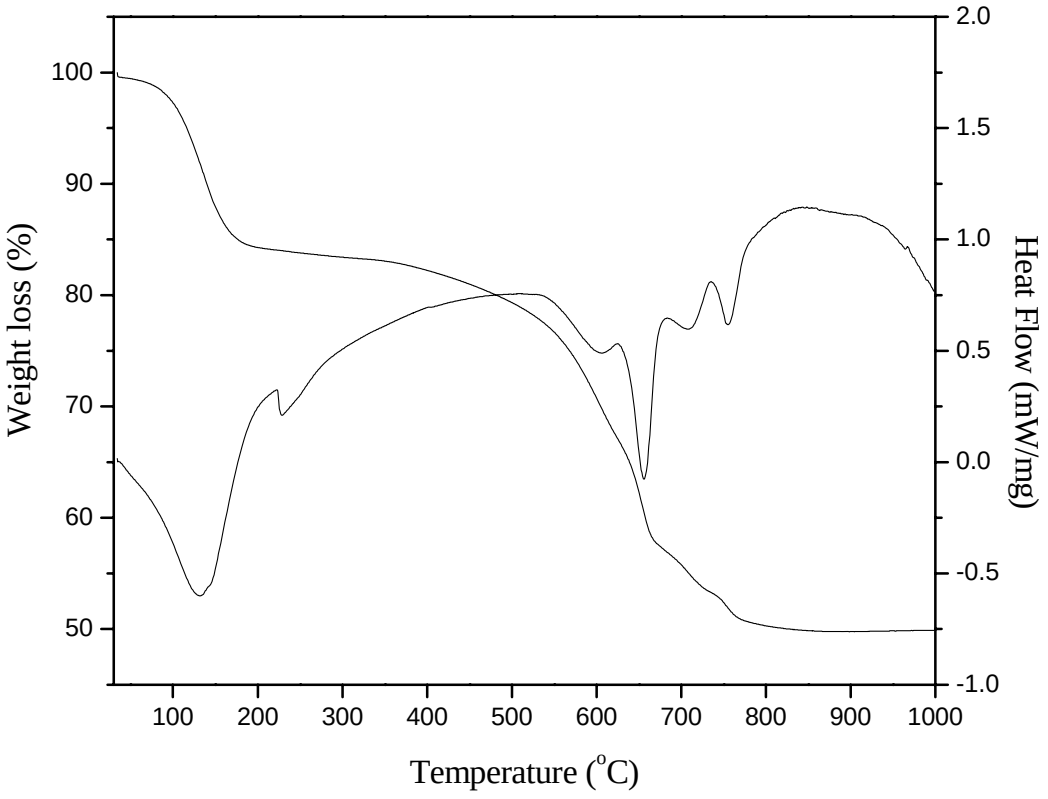

Fig.7. DSC-TG plot of T-BGC gel powder

DSC-TG curve (fig.7) for TEOS based gel powder (T-BGC) shows similar behavior as for RHS based, Soda-lime- silicate gel powder. It also has three stages of weight loss in same temperature range as above. The peak at 227^{o}C may be due to crystallization of sodium nitrate or/and calcium nitrate. Although, the presence of calcium nitrate could not be detected by XRD analysis which may be due to its minute amount.

XRD of NS-BGC and T-BGC samples

Fig.8(a) shows XRD pattern of gel powder NS-BGC gel powder. Pattern shows the presence of crystalline peaks for $NaNO_3$ for silicate gel.

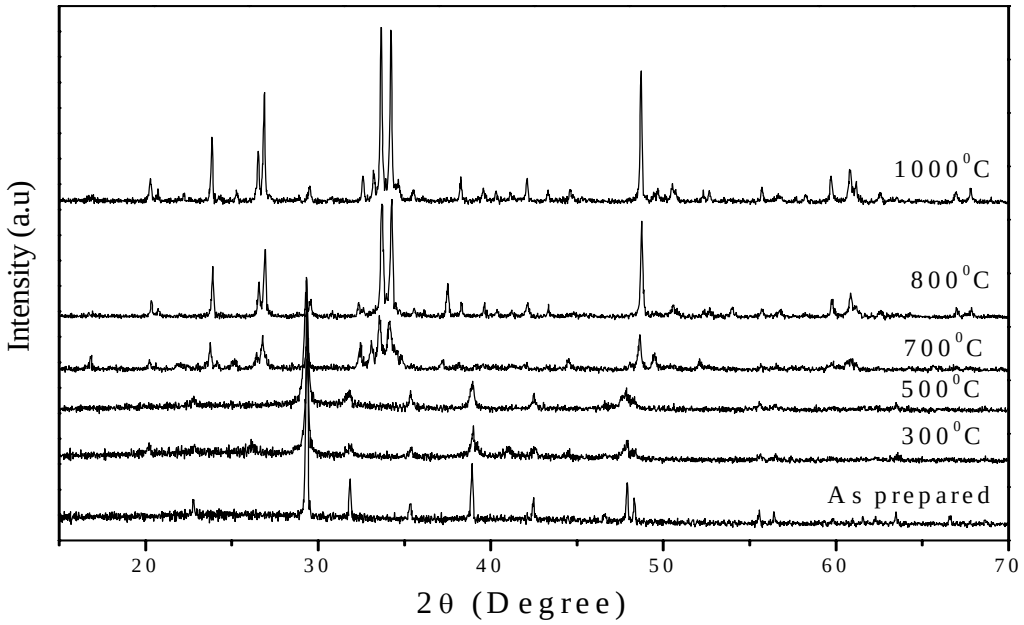

Fig.8. XRD pattern of NS-BGC sample heated at different temperature

Whereas fig 9(a) shows the XRD pattern of gel powder synthesized from TEOS. It contains mainly NaNO3 crystalline phase {JCPDS 76-2243} (corresponds to all peak) and amorphous gel phase.

Fig.8(b) shows the pattern of gel powder calcined at 300^{0}C for 2 hours (hrs). It shows that Sodium Nitrate, calcium Nitrate and amorphous material are present in the sample. In the raw powder Ca was present in Silica gel structure. When the gel was heated at 300^{0}C Ca precipitated as Calcium Nitrate from gel structure to some extent.

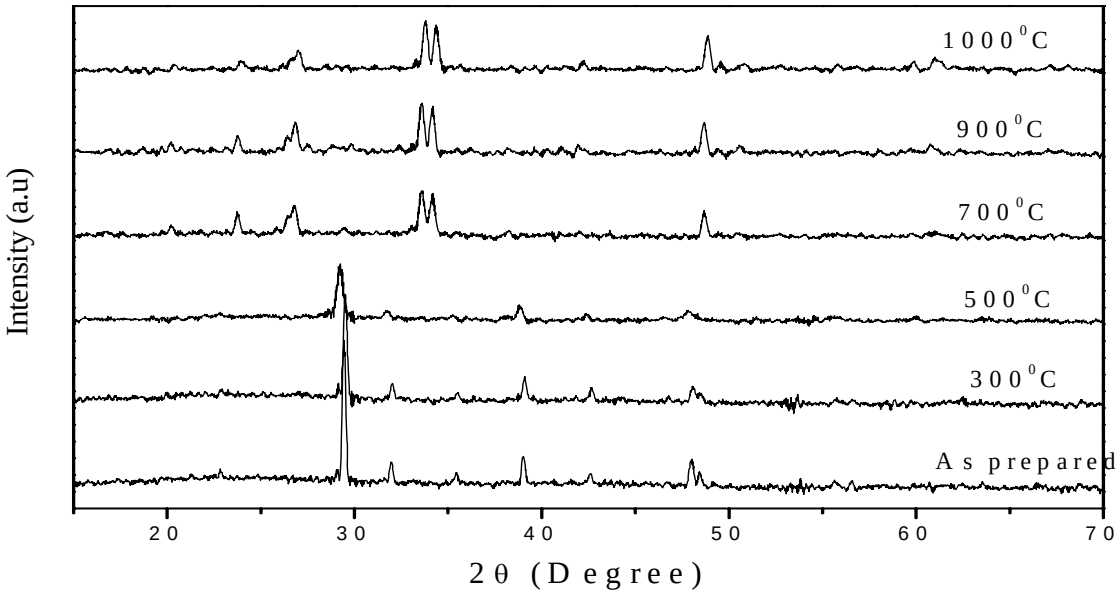

Fig. 9. XRD pattern of T-BGC sample heated at different temperature

Whereas, T-BGC powder calcined at 300^{o}C and 500^{o}C has same phase as its raw powder (fig.9(b) and fig.9(c)).

However $Ca(NO_3)_2$ was not present in the powder sample(fig 8(c)) which was heat treated at 500^{0}C for 2 hrs. This may be due to decomposition of $Ca(NO_3)_2$ by heat treatment. The TG-DSC plot also shows a weight loss in the temperature range (200^{o}C-500^{o}C) due to that decomposition. Sodium Nitrate decomposition and reaction occurred after heat treating the powder at 700^{0}C for 2 hrs. The sample pattern (fig.8(d)) shows that there is formation of Sodium Calcium Silicate with two different crystalline phases majority being $Na_6Ca_3Si_6O_{18}$ (JCPDS 77-2189) and second one is $Na_2Ca_2Si_2O_7$ (JCPDS 10-0016).

In case of T-BGC, XRD pattern (fig 9(d)) shows the existence of $Na_2CaSi_3O_6$ (JCPDS 12-0671) along with $Na_2Ca_3Si_6O_{18}$.

The XRD pattern (fig 8(e)) of NS-BGC sample, sintered at 800^{o}C, shows the presence of $Na_6Ca_3Si_6O_{18}$ and $Na_2Ca_3Si_6O_{16}$. Whereas XRD pattern (fig 9(e)) of T-BGC sample, at this temperature, show the existence of $Na_4Ca_4Si_6O_{16}$ (combeite) (JCPDS 75-1686) as major phase and minor phase was $Na_2Ca_3Si_6O_{16}$.

The two Sodium Calcium Silicate phase of NS-BGC sample reacts with each other to form a another single Sodium Calcium Silicate phase (fig.8(f)) with chemical formula $Na_4Ca_4Si_4O_{18}$

(JCPDS 75-1687) upon heat treatment at 900^{o}C for 2hrs however there was minor (~5%) free CaO phase was found in the sample.

At 1000^{0}C XRD pattern (fig.8 (g)) of NS-BGC sample shows the presence of 50% each of $Na_6Ca_3Si_6O_{18}$ and $Na_2Ca_3Si_6O_{16}$ was found.

The XRD pattern of T-BGC samples upon heat treatment at 900^{o}C shows the presence of $Na_6Ca_3Si_6O_{18}$ (JCPDS 77-2189) as major phase and second phase is $Na_2Ca_3Si_6O_{16}$. Whereas upon heat treatment at 1000^{o}C, XRD pattern shows Combeite phase having chemical formula $Ca_3Na_{15.78}(Si_6O_{12})$. There was incipient melting at this temperature on surface of sample and blotting of sample occurred due to this.

XRD of SBF treated NS-BGC and T-BGC samples

Fig.10(a) shows XRD pattern of 3 days SBF treated NS-BGC sample which indicates the formation of carbonated HAP (Hydroxyapatite) $[Ca_{10}(PO_4)_3(CO_3)_3(OH)_2]$ (JCPDS 19-0272) and hydrated Ca-hydrogen-phosphate phase upon the surface of samples. There were no peaks corresponding to any of Sodium Calcium Silicate phase. Amorphous phase content of samples also increased. This is due to the dissolution of glass ceramics in SBF solution which releases Sodium and Calcium ion fom its Silica network glass structure. That is why pH of solution increases and solution became supersaturated with respect to Na and Ca ion concentration which helps in precipitation of Ca as a form of Calcium-hydrogen-phosphate and carbonated HAP upon the surface of glass-ceramics. In actual, the glass-ceramics may now be considered as a glassy material because there is no crystalline phase of original ceramic body.

Although, there were no such peaks corresponding to apatite layer formation in T-BGC sample after 3 days of SBF treatment. XRD pattern of sample was quite similar to that of original, untreated sample. Whereas after 7 days of treatment with SBF, XRD pattern shows the presence of Sodium calcium silicate and Carbonated hydroxyapatite

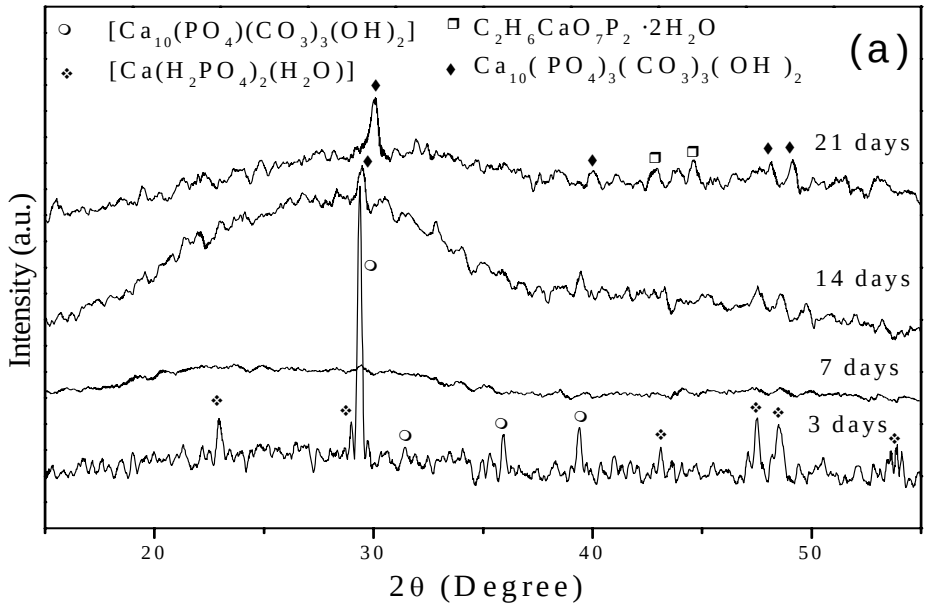

Fig.10. XRD pattern of SBF treated NS-BGC samples

In case of NS-BGC sample, after 7 days of treatment with SBF, all peaks in XRD were corresponding to carbonated hydroxyapatite [$Ca_{10}(PO_4)_3(CO_3)_3(OH)_2$].

The transformation to glassy material by dissolution of ions is more evident in 14 days. The sample shows again the presence of carbonated HAP.

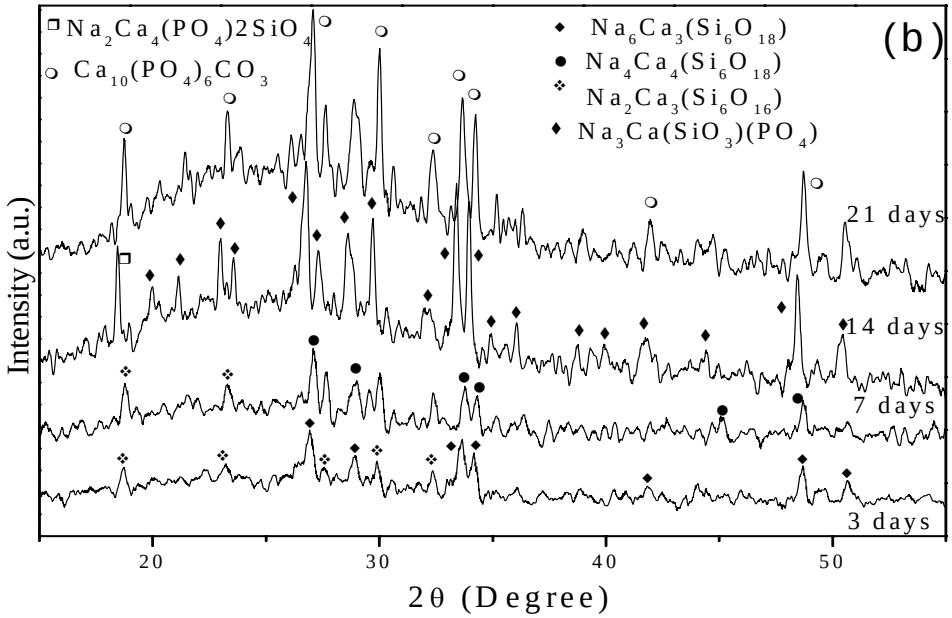

Fig. 11. XRD patterns of glass ceramics after immersion in SBF for different days. (a) NS-BGC Specimen (BD~ 1.51, AP~20%) and (b) T-BGC specimen (BD~ 1.8, AP~13%).

phosphate upon glass matrix. In T-BGC sample, after 14 days of soaking, $Na_3Ca(SiO_3)(PO_4)$ along with minute amount of Na2Ca4(PO4)2SiO_4 phases were found.

After 21 days of soaking in SBF, RHA synthesized sample had, carbonated hydroxyapatite $[Ca_{10}(PO_4)_3(CO_3)_3(OH)_2]$ and $C_2H_6CaO_7P_2.2H_2O$ phases, grown on its surface. Whereas all peaks of T-BGC sample were identified as $Ca_{10}(PO_4)_6CO_3$.

SEM and EDXA of NS-BGC and T-BGC sample

The fig is SEM image of pure NS- BGC, sintered at 800^oC. It shows the presence of silica in glassy phase, the rod like structure. EDXA of this sample clearly verifies that it contains Si,O,Ca and Na as it was taken in our composition. These samples were submerged in SBF for bioactivity test which shows the presence of Mg, C and P on its surface indicating formation of apatite and carbonated hydroxyapatite layer. The composition and concentration varied with time for which it was kept submerged in SBF.

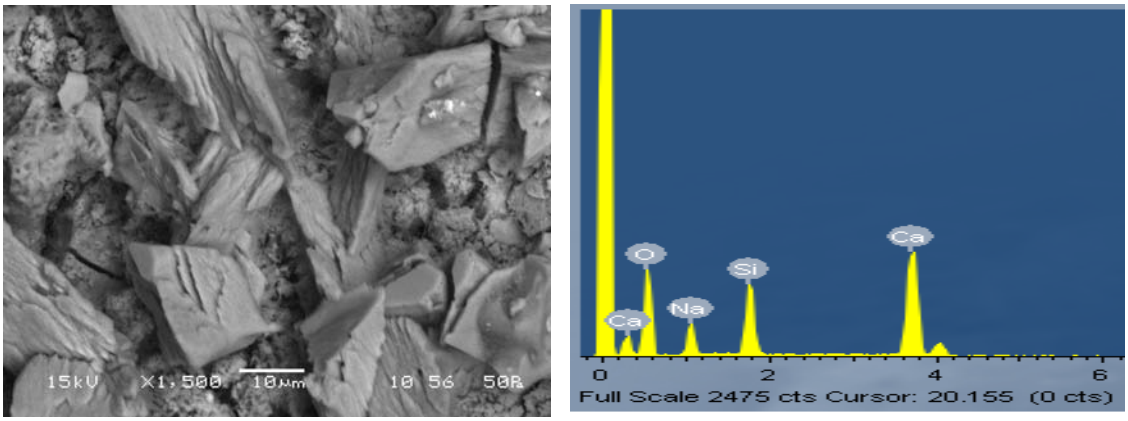

Fig.12. SEM and EDX image of pure NS-BGC sample

The fig shows surface morphology of NS- BGC after immersion in SBF for 3 days. Its surface has Mg and P with 0.61 and 8.91 wt% along with above composition which was derived from SBF solution. The XRD report also verifies the presence of (Hydroxyapatite) $[Ca_{10}(PO_4)_3(CO_3)_3(OH)_2]$ and hydrated Ca-hydrogen-phosphate . Due to formation of this layer, which covered the sample surface, Wt % of Si and O has decreased which is major component of sample. Average grain size of Hydroxyapatite was found to be 0.98 micrometer and Ca/P ratio(wt/wt) was calculated to be 2.97.

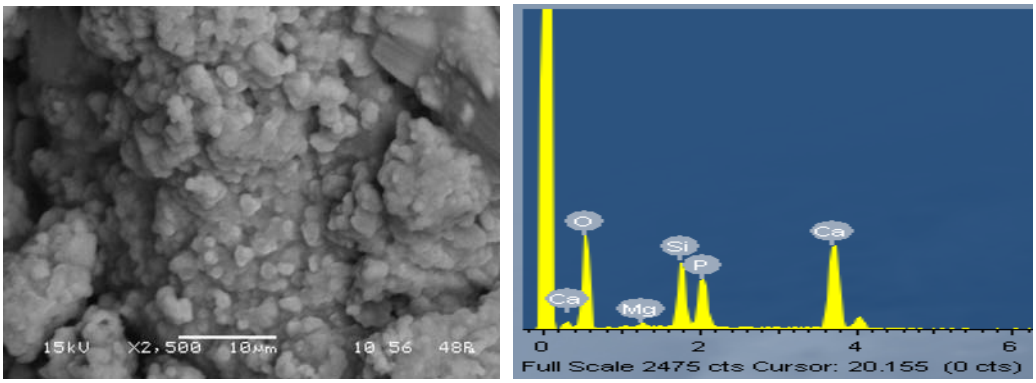

Fig.13. SEM and EDX image of NS-BGC sample after immersion in SBF for 3 days

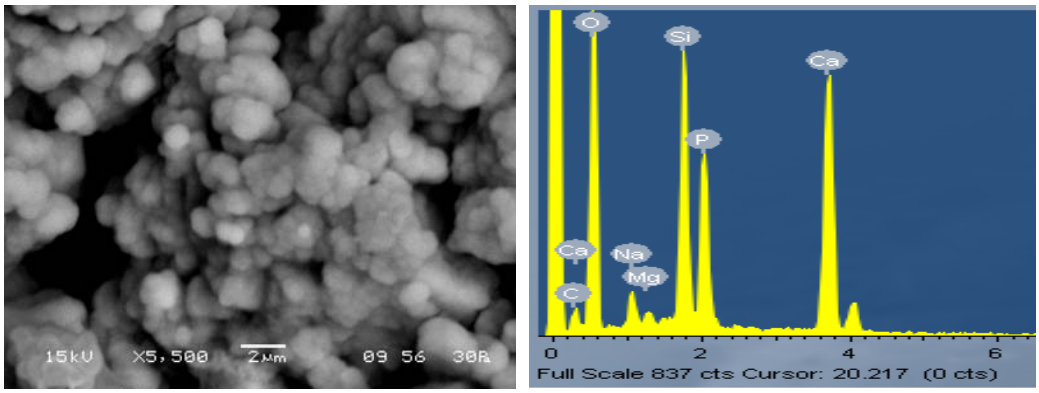

Fig.14. SEM and EDX image of NS-BGC sample after immersion in SBF for 7 days

When NS- BGC sample was kept in SBF solution for 7 days, Carbonated Hydroxyapatite phase was formed denser than that in 3 days which is identified in XRD report of sample. The EDX analysis also shows the presence of C on its surface. Ca/P ratio has decreased to 2.37 from 2.97. The wt % of Si and O has further more decreased due to formation of denser and spherical Carbonated Hydroxyapatite on the surface. The grain size of this Carbonated Hydroxyapatite was found to b 1.06 micrometer which is larger than that in 3days, indicating grain growth.

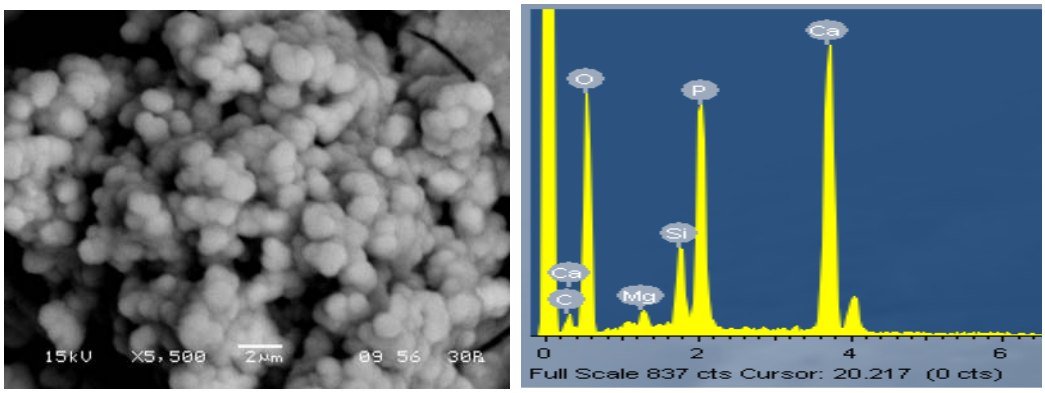

Fig.15. SEM and EDX image of NS-BGC sample after immersion in SBF for 14 days

Fig shows the SEM image of NS- BGC sample kept immersed in SBF for 14 days. Comparing the images of 7days and 14 days clearly shows very rapid growth of carbonated HAP and Calcium-hydrogen-phosphate upon glass matrix phases verified by XRD peaks. EDX analysis of these two samples shows drastic decrease in Si content of sample from 9.11 to 3.81 wt % and rise in P content from 8.74 to 13.33 wt %. The average grain size of newly formed phases containing Calcium-hydrogen-phosphate were found to be1.09 micrometer which is even larger than 7 days. Ca/P ratio of surface was found as 2.11 which shows decreasing order of ratio with increasing soaking time.

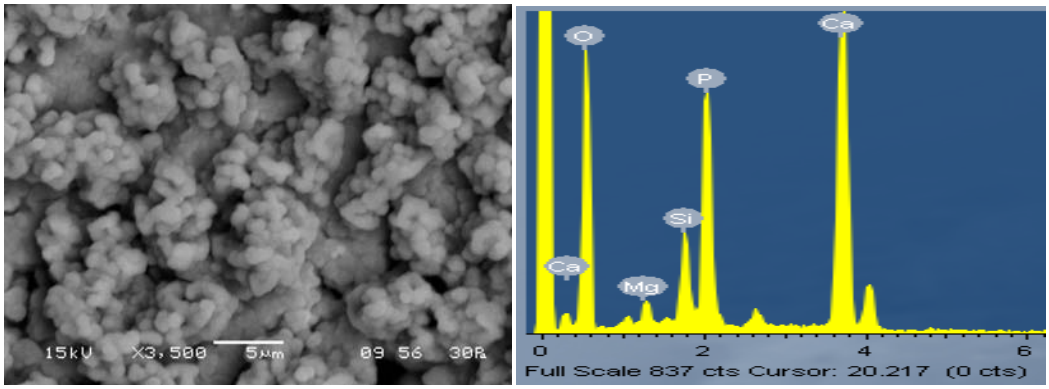

Fig.16. SEM and EDX image of NS-BGC sample after immersion in SBF for 21 days

SEM report (fig) of NS- BGC sample after 21 days soaking in SBF shows the presence of carbonated hydroxyapatite [$Ca_{10}(PO_4)_3(CO_3)_3(OH)_2$] and $C_2H_6CaO_7P_2.2H_2O$ phases which is similar to sample treated for 14 days. Silica content has further decreased to 3.43 wt %. The average grain size remained almost constant as 1.10 micrometer. Ca/P ratio of surface was found as 2.10 showing similarity with sample treated for 14 days. The constant behavior of the 14 days and 21 days sbf treated sample indicates the completion of apatite layer formation.

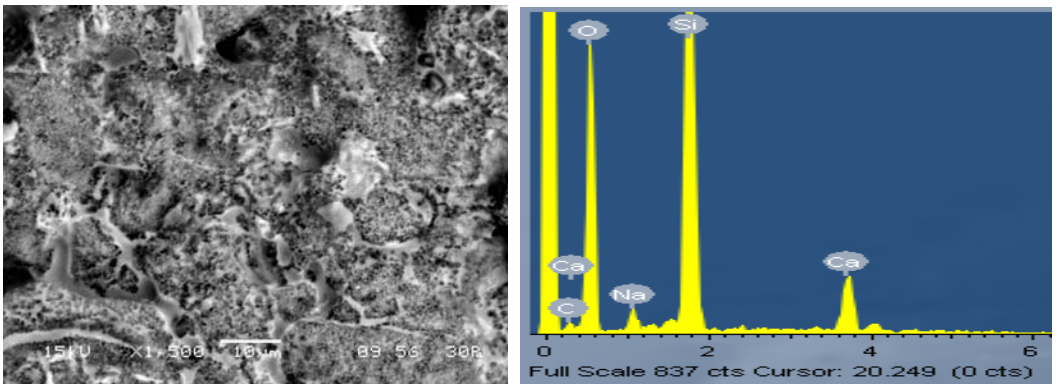

Fig.17. SEM and EDX image of T-BGC sample after immersion in SBF for 3 days

The fig shows surface morphology of T- BGC, sintered at 800^{o}C, after immersion in SBF for 3 days. Its surface doesn't have any apatite layer formation on it as indicated by EDX and XRD. The sample contain Si-36.82%,Ca-7.10%,O-49.99%,Na-1.48% along with C having 4.61 wt%. as with NS-BGC, apatite layer formation occurred on T-BGC sample but the rate of formation was slower than NS-BGC. Reduced amount of Na and Ca is due to its dissolution into SBF solution.

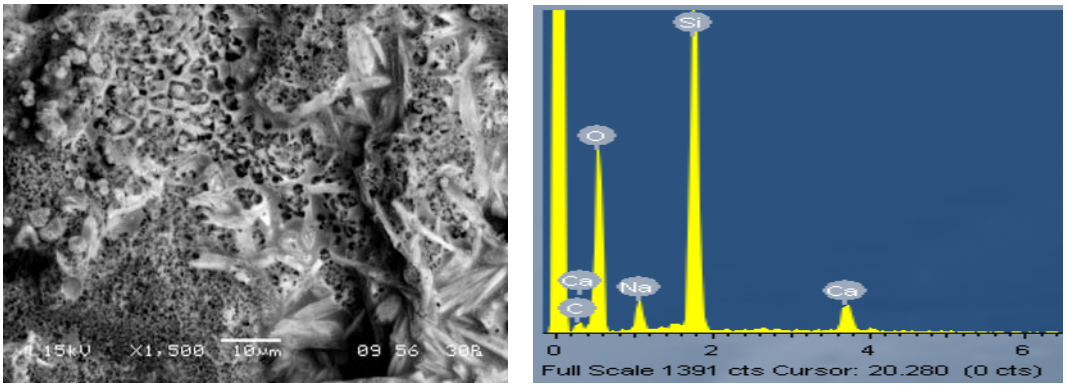

Fig.18 SEM and EDX image of T-BGC sample after immersion in SBF for 7 days

Even after keeping the T-BGC sample (Fig. 18) in SBF for 7 days , there was no trace of apatite layer formation. Increase in the amount of C and O from 4.61 wt % to 5.29 wt% and from 49.99wt% to 53.75wt% indicates the deposition of CO_3^-on the surface of sample.

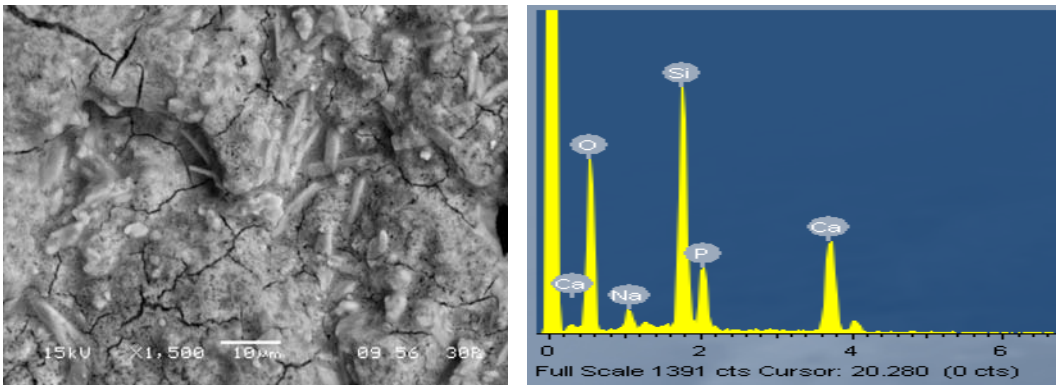

Fig.19. SEM and EDX image of T-BGC sample after immersion in SBF for 14 days

When T-BGC sample was left in SBF for 14 days, presence of P was indicated by EDXA and the phase formed was found to be $Na_3Ca(SiO_3)(PO_4)$ as major phase and minute amount of $Na_2Ca_4(PO4)2SiO_4$ was also found as shown by XRD. Increase in the amount of Ca from 7.10 to 16 wt % and presence of P (7.62 wt %) indicates precipitation calcium phosphate along with Na whose amount has increased to 2.41 wt %. Due to formation of this layer on glass ceramic surface, the Si content in EDX has reduced to 20 wt %.

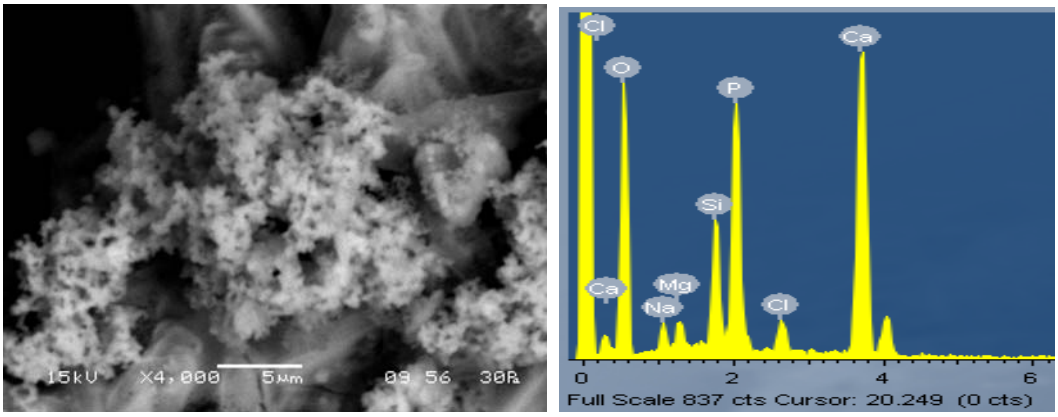

Fig.20. SEM and EDX image of T-BGC sample after immersion in SBF for 21 days

The fig corresponds to T-BGC sample treated with SBF for 21 days. It shows high density of apatite layer formation. High peak of P, indicated by EDX, shows increased amount of P on sample surface. Phases, as found by XRD, are $Ca_{10}(PO_4)_6CO_3$.

In-vitro degradation:

In order to study the dissolution/reprecipitation features of glass-ceramics, Tris buffer solutions was chosen because, Tris is the plain buffering agent used in most SBF preparations [21]. Tris solutions, whose use has been suggested also by Hench [37], do not contain ions and thus represent, for a bioactive material, maximum solubility and minimum reprecipitation activity. Pure Tris was dissolved in distilled water to obtain a concentration of 6.1 gpl. The solution pH was lowered to 8 by acidifying with a solution of 1 M HCl.

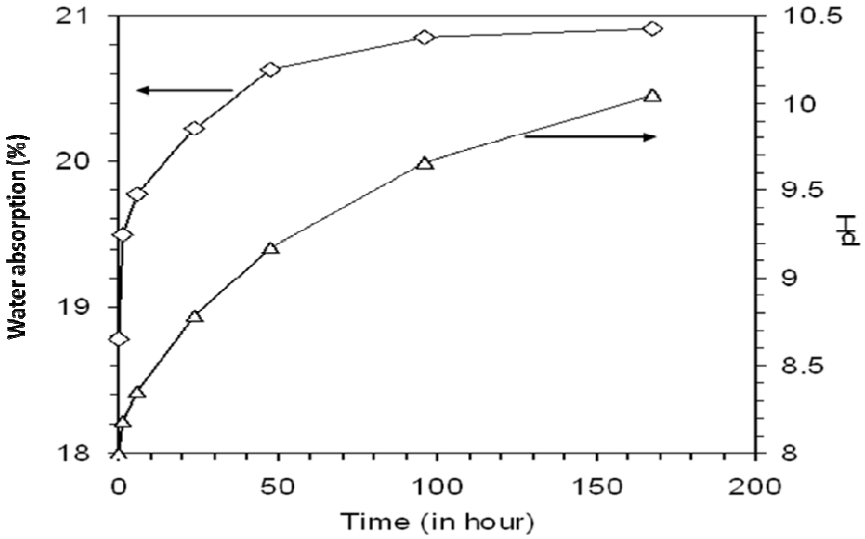

Fig. 21. Water absorption of NS-BGC sample and pH change of Tris buffer on immersion

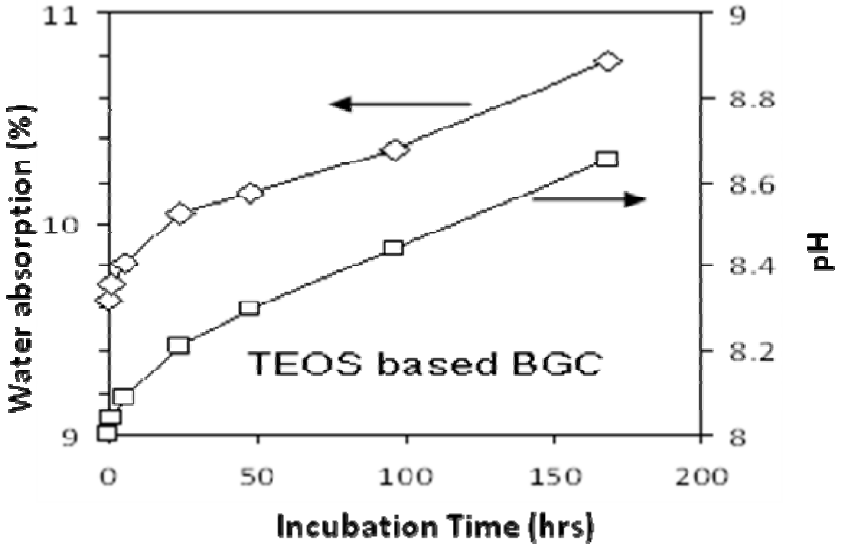

Fig. 21. Water absorption of NS-BGC sample and pH change of Tris buffer on immersion

Conclusion

The main conclusions of this study can be summarized as follows:

(i) Highly bioactive glass ceramics composed of SiO_2–CaO–Na_2O have been synthesized using rice husk ash waste material as a source of silica.

(ii) Low-temperature sol–gel processing is an appropriate method for the preparation of the bio-glass ceramics.

(iii) HAP formation is observed within 3 days of reaction for NS-BGC whereas, in the case of T-BGC, times between 14 and 21 days of reaction are required.

(iv) During dissolution reactions, the increment of pH value (mainly caused by Na and Ca release) is higher for NS-BGC than T-BGC.

References:

1. L. L. HENCH, *J. Amer. Ceram. Soc*. **74** (7) (1991) 1487.

2. T. KOKUBO, H. KUSHITAI, C. OHTSUKI, S . SAKKA and T.YAMAMURO, *J. Mater. Sci. Mat. Med*. **3** (1992) 79.

3. L. L. HENCH, *Amer. Ceram. Soc. Bull*. **77** VII (1998) 67.

4. L. L. HENCH, R. J. SPLINTER, W. C. ALLEN and T. K. GREENLEE, J. Biomed. Mater. Res. 2 (1971) 117

5. H. OONISHI, L. L. HENCH, J. WILSON, F. SUGIHARA, E. TSUJI, M. MATSUURA, S. KIN, T. YAMAMURO and S. MIZOKAWA,

J. Biomed. Mater. Res. 51 (2000) 37

6. P. DUCHEYNE and J. M. CUCKLER, Rev. Clin. Ortho. Rel. Res. 277 (1992) 102

7. M. VALLET-REGI`, J. Chem. Soc. Dalton Trans. 5 (2001) 97

8. E. VERNE` , M. BOSETTI, C. VITALE-BROVARONE, C. MOISESCU, F. LUPO, S. SPRIANO and M. CANNAS, Biomaterials 23 (2002) 3395

9. E. VERNE` , R. DEFILIPPI, G. CARL, C. VITALE-BROVARONE and P. APPENDINO, J. Eur. Cer. Soc. 23 (2003) 675

10. C. Vitale-Brovarone, S. Di Nunzio, O. Bretcanu, E. Verne`, J. Mat. Sci. Mat. Med. 15 (2004) 209

11. E. VERNE` , F. VALLES, C. VITALE-BROVARONE, S. SPRIANO and C. MOISESCU, J. Eur. Cer. Soc. 24 (2004) 2699

12. C. VITALE-BROVARONE and E. VERNE` , J. Mat. Sci. Mat. Med. 16 (2005) 863

13. J. E. GOUGH, J. R. JONES and L. L. HENCH, Biomaterials 25 (2004) 2039

14.I. JUN, Y. KOH and H. KIM, J. Am. Cer. Soc. 89 (2006) 391

15. M. M. PEREIRA, J. R. JONES and L. L. HENCH, Adv. App. Cer. 104 (2004) 35

16. T. KOKUBO, H. KUSHITANI and S. SAKKA, J. Biomed. Mater. Res. 24 (1990) 721

17. W. K. RAMP, L. G. LENZ and K. K. KAYSINGER, Bone Miner. 24 (1994) 59

18. K. K. KAYSINGER and W. K. RAMP, J. Cell Biochem. 68 (1998) 83

19. A. BRANDAO-BURCH, J. C. UTTING, I. R. ORRISS and T. R. ARNETT, Calcif. Tissue Int. 77 (2005) 167

20. K. K. FRICK, L. JIANG and D. A. BUSHINSKY, Am. J. Physiol. 272 (1997) C1450

21. A. EL-GHANNAM, P. DUCHEYNE and I. SHAPIRO, Biomaterials 18 (1997) 295

22. Blaker JJ, Nazhat SN, Boccaccini AR. Development and characterization of silver-doped bioactive glass-coated sutures for tissue engineering and wound healing applications. Biomaterials 2004; 25:1319–29.

23. Saravanapavan P, Gough JE, Jones JR, Hench LL. antimicrobial macroporous gel glasses: dissolution and cytotoxicity. Key Eng Mater 2004; 254–256:1087–90.

24. H.S. Ryu, J.H. Seo, H. Kim, K.S. Hong, H.J. Park, D.J. Kim, J.H. Lee, D.H. Lee, B.S. Chang, C.K. Lee, Bioceramics 15, Trans Tech Publications Ltd., Zurich-Uetikon, 2003, p. 261.

25. M. Vallet-Regi, C.V. Ragel, A.J. Salinas, Eur. J. Inorg. Chem. (2003) 1029–1042.

26 Kasuga T, Abe Y. Calcium phosphate invert glasses with soda and titania. J Non-Cryst Solids 1999;243:70–4.

27. Zhang Y, Santos JD. Crystallization and microstructure analysis of calcium phosphate-based glass ceramics for biomedical applications. J Non-Cryst Solids 2000; 272:14–21.

28. Kumar S, Vinatier P, Levasseur A, Rao KJ. Investigations of structure and transport in lithium and silver borophosphate glasses. J Solid State Chem 2004;177:1723–37.

29. Saravanapavan P, Hench LL. Low temperature synthesis, structure and bioactivity of gel derived glasses in the binary CaO–SiO2 system. J Biomed Mater Res 2001;54:608–18.

30. Sepulveda P, Jones JR, Hench LL. Characterization of melt derived 45S5 and sol gel derived 58 S bioactive glasses. J Biomed Mater Res 2001;58:734–40.

31. Perez-Pariente J, Balas F, Roman J, Salinas AJ, Vallet-Reg M. Influence of composition and surface characteristics on the in vitro bioactivity of SiO2–CaO–P2O5–MgO sol–gel glasses. J Biomed Mater Res 1999;47:170–6. A. Balamurugan et al. / Acta Biomaterialia 3 (2007) 255–262 261

32. Leonelli C, Lusvardi G, Malavasi G, Menabue L, Tonelli M. Synthesis and characterization of cerium-doped glasses and in vitro evaluation of bioactivity. J Non-Cryst Solids 2003;316:198–216.

33. Hill RG, Stamboulis A, Law RV, Clifford A, Towler MR, Crowley C. The influence of strontium substitution in fluorapatite glasses and glass-ceramics. J Non-Cryst Solids 2004;336:223–9.

34. Saranti A, Koutselas I, Karakassides MA. Bioactive glasses in the system CaO–B2O3–P2O5: preparation, structural study and in vitro evaluation. J Non-Cryst Solids 2006; 352:390–8.

35. Kokubo T, Takadama H. How useful is SBF in predicting in vivo bone bioactivity? Biomaterials 2006;27:2907–15.

36. Kim CY, Clark AE, Hench LL. Early stages of calcium phosphate layer formation in bioglasses. J Non-Cryst Solids 1989;113:195–202.

37. Kim CY, Clark AE, Hench LL. Early stages of calcium phosphate layer formation in bioglasses. J Non-Cryst Solids 1989;113:195–202.